



HAL
open science

Transgenerational metabolomic fingerprints in mice ancestrally exposed to the obesogen TBT

Raquel Chamorro-García, Nathalie Poupin, Marie Tremblay-Franco, Cécile Canlet, Riann Egusquiza, Roselyne Gautier, Isabelle Jouanin, Bassem M Shoucri, Bruce Blumberg, Daniel Zalko

► To cite this version:

Raquel Chamorro-García, Nathalie Poupin, Marie Tremblay-Franco, Cécile Canlet, Riann Egusquiza, et al.. Transgenerational metabolomic fingerprints in mice ancestrally exposed to the obesogen TBT. *Environment International*, 2021, 157, 10.1016/j.envint.2021.106822 . hal-03335779

HAL Id: hal-03335779

<https://hal.inrae.fr/hal-03335779v1>

Submitted on 6 Sep 2021

HAL is a multi-disciplinary open access archive for the deposit and dissemination of scientific research documents, whether they are published or not. The documents may come from teaching and research institutions in France or abroad, or from public or private research centers.

L'archive ouverte pluridisciplinaire **HAL**, est destinée au dépôt et à la diffusion de documents scientifiques de niveau recherche, publiés ou non, émanant des établissements d'enseignement et de recherche français ou étrangers, des laboratoires publics ou privés.



Distributed under a Creative Commons Attribution - NonCommercial - NoDerivatives 4.0
International License



Transgenerational metabolomic fingerprints in mice ancestrally exposed to the obesogen TBT

Raquel Chamorro-García^{a,1}, Nathalie Poupin^b, Marie Tremblay-Franco^b, Cécile Canlet^b,
Riann Egusquiza^{c,2}, Roselyne Gautier^b, Isabelle Jouanin^b, Bassem M. Shoucri^{a,3},
Bruce Blumberg^{a,c,d,*}, Daniel Zalko^{b,*}

^a Department of Developmental and Cell Biology, 2011 Biological Sciences 3, University of California, Irvine 92697-2300, USA

^b Toxalim (Research Center in Food Toxicology), Université de Toulouse, INRAE, ENVT, INP-Purpan, UPS, 31300 Toulouse, France

^c Department of Pharmaceutical Sciences, University of California, Irvine, USA

^d Department of Biomedical Engineering, University of California, Irvine, USA

ARTICLE INFO

Handling Editor: Adrian Covaci

Keywords:

Tributyltin
Endocrine disruptor
Metabolic disruptor
Transgenerational effects
Metabolomics
Obesogen

ABSTRACT

Background: Endocrine disrupting chemicals (EDCs) contribute to the etiology of metabolic disorders such as obesity, insulin resistance and hepatic dysfunction. Concern is growing about the consequences of perinatal EDC exposure on disease predisposition later in life. Metabolomics are promising approaches for studying long-term consequences of early life EDC exposure. These approaches allow for the identification and characterization of biomarkers of direct or ancestral exposures that could be diagnostic for individual susceptibility to disease and help to understand mechanisms through which EDCs act.

Objectives: We sought to identify metabolomic fingerprints in mice ancestrally exposed to the model obesogen tributyltin (TBT), to assess whether metabolomics could discriminate potential trans-generational susceptibility to obesity and recognize metabolic pathways modulated by ancestral TBT exposure.

Methods: We used non-targeted ¹H NMR metabolomic analyses of plasma and liver samples collected from male and female mice ancestrally exposed to TBT in two independent transgenerational experiments in which F3 and F4 males became obese when challenged with increased dietary fat.

Results: Metabolomics confirmed transgenerational obesogenic effects of environmentally relevant doses of TBT in F3 and F4 males, in two independent studies. Although females never became obese, their specific metabolomic fingerprint evidenced distinct transgenerational effects of TBT in female mice consistent with impaired capacity for liver biotransformation.

Discussion: This study is the first application of metabolomics to unveil the transgenerational effects of EDC exposure. Very early, significant changes in the plasma metabolome were observed in animals ancestrally exposed to TBT. These changes preceded the onset of obesogenic effects elicited by increased dietary fat in the TBT groups, and which ultimately resulted in significant changes in the liver metabolome. Development of metabolomic fingerprints could facilitate the identification of individuals carrying the signature of ancestral obesogen exposure that might increase their susceptibility to other risk factor such as increased dietary fat.

1. Introduction

39.8% of the U.S. population was estimated to be clinically obese with the burden falling disproportionately on African-American and

Hispanic populations. ~47% of African- and Hispanic Americans are obese including >50% of women (Hales et al., 2017). Latest estimates from the WHO for European Union countries indicate that 30–70% of adults are overweight, and 10–30% obese (World Health Organization,

* Corresponding authors at: Department of Developmental and Cell Biology, 2011 Biological Sciences 3, University of California, Irvine 92697-2300, USA (B. Blumberg).

E-mail addresses: blumberg@uci.edu (B. Blumberg), daniel.zalko@inrae.fr (D. Zalko).

¹ Present address: Department of Microbiology and Environmental Toxicology, University of California, Santa Cruz, USA.

² Present address: DTxPharma, San Diego, CA 92121, USA.

³ Present address: School of Medicine, University of California, Los Angeles, CA 90024, USA.

<https://doi.org/10.1016/j.envint.2021.106822>

Received 6 April 2021; Received in revised form 9 August 2021; Accepted 9 August 2021

Available online 26 August 2021

0160-4120/© 2021 The Authors.

Published by Elsevier Ltd.

This is an open access article under the CC BY-NC-ND license

(<http://creativecommons.org/licenses/by-nc-nd/4.0/>).

2020). Positive energy balance and genetics are commonly ascribed as primary causes of obesity. However, those factors only explain part of the cases (Locke et al., 2015; Ludwig et al., 2018). Since obesity and related diseases are very costly to society, impair quality of life and have many psychological consequences in addition to physical disabilities, identifying all the factors that predispose individuals to obesity and the mechanisms through which these factors act is a critical challenge that must be overcome to reverse the worldwide growth of obesity.

A growing body of evidence shows that environmental endocrine-disrupting chemicals (EDCs) may play an important role in the current obesity trends (reviewed in Heindel and Blumberg, 2019). EDCs are exogenous chemicals that interfere with the function of natural hormones and therefore, can lead to various endocrine diseases such as cancer and reproductive dysfunction (Gore et al., 2015; Zoeller et al., 2012). Obesogens are a subset of EDCs that contribute to weight gain and obesity by altering the number, size and/or function of white adipocytes, the production and/or function of thermogenic brown and beige/brite adipocytes, adipocyte homeostasis, the control of appetite and satiety or metabolic setpoints of the organisms (reviewed in Heindel and Blumberg, 2019). Examples of obesogens include organotin compounds such as tributyltin (TBT), dibutyltin (DBT) and triphenyltin (TPT) (Chamorro-García et al., 2018; Grun et al., 2006; Kanayama et al., 2005; Li et al., 2011; Milton et al., 2017; Shoucri et al., 2018), bisphenols such as bisphenol A (BPA), halogenated BPA analogs (Riu et al., 2014), diethylstilbestrol (Newbold et al., 2009) and dichlorodiphenyltrichloroethane (DDT) (Cano-Sancho et al., 2017; Skinner et al., 2013). However, the mechanisms through which most obesogens act, *in vivo*, largely remain unclear.

TBT activates both the 9-cis retinoic acid receptor (RXR) and peroxisome proliferator activated receptor gamma (PPAR γ) (Grun et al., 2006; Kanayama et al., 2005; Li et al., 2011). These nuclear receptors act as a heterodimer that is required for the commitment (Shoucri et al., 2017) and terminal differentiation of white adipocytes, respectively (Tontonoz and Spiegelman, 2008). PPAR γ was also demonstrated to be a target for halogenated bisphenols (Riu et al., 2014). Multipotent mesenchymal stromal stem cells (MSCs) and murine 3T3-L1 pre-adipocytes induced to differentiate into adipocytes by exposure to TBT generated dysfunctional adipocytes with increased expression of pro-inflammatory markers, low levels of the metabolically healthy adipokine adiponectin, decreased capability for glucose uptake (Regnier et al., 2015; Shoucri et al., 2018) and impaired ability to undergo “browning” into beige/brite adipocytes (Kim et al., 2018; Shoucri et al., 2018).

In vivo studies in rodents showed that adult exposure to TBT led to non-alcoholic fatty liver disease (NAFLD) in males. In parallel, an alteration in the hypothalamus-pituitary-gonadal axis in females (Sena et al., 2017; Zuo et al., 2011), was consistent with an overall alteration of the endocrine system. *In utero* TBT exposure resulted in increased fat storage, non-alcoholic fatty liver and a bias of MSCs toward the adipogenic pathway at the expense of the bone pathway in the offspring (Chamorro-García et al., 2013; Chamorro-García et al., 2018; Grun et al., 2006; Kirchner et al., 2010; Watt and Schlezinger, 2015; Watt et al., 2018). Interestingly, effects of prenatal TBT exposure were transmitted to subsequent generations. The phenotype was observed in F1 and F2 generations (which were directly exposed to TBT) and also in F3 and F4 generations that were not directly exposed to TBT, an example of transgenerational inheritance (Chamorro-García et al., 2013; Chamorro-García et al., 2017). Targeted plasma analyses showed that (F3-F4) male mice ancestrally exposed to TBT had increased leptin levels, whereas other hormones involved in metabolic regulation such as adiponectin, ghrelin or insulin were unchanged (Chamorro-García et al., 2017).

In vivo evidence of the impact of obesogens on selected biochemical parameters is a necessary prerequisite to assess the metabolic effects of these compounds, but targeted analyses are limited in their ability to unravel mechanisms of action or to unveil early biomarkers of effects. Information obtained from targeted analyses does not extensively examine the metabolomic profile of individuals; therefore, it is

inherently incomplete and insufficient to identify shifts in biochemical pathways responsible for metabolic modulation.

Non-targeted metabolomics based on spectral nuclear magnetic resonance (NMR) and/or mass spectrometry (MS) analyses allows the study of hundreds of endogenous and exogenous small metabolites and lipids in biological samples. Combined with multivariate statistical analyses, non-targeted metabolomics enables the unbiased identification of “discriminant” endogenous metabolites that significantly vary in their concentration levels according to exposure conditions and constitute a “metabolic fingerprint” of exposure and its effects. Combined with systems biology (bioinformatics), metabolomics also paves the way for the modeling of functional metabolic networks, allowing a better understanding of pathways involved in metabolic modulation consequent to EDC exposure. Metabolomics may contribute to the early diagnosis of human disease (Emwas et al., 2013). For our studies, a necessary first step is the unambiguous demonstration of a lasting impact of obesogen exposure on metabolism.

We pioneered the use of metabolomics in the field of EDC science, by demonstrating that the metabolome of mice born from dams exposed to low doses of BPA during gestation/lactation was significantly and durably impaired in the F1 generation (Cabaton et al., 2013). Characteristic “metabolomic fingerprints” were apparent in whole body extracts of newborns and later in specific tissues such as the liver and the brain (Cabaton et al., 2013; Zalko et al., 2016). Perinatal effects of BPA in rats were also examined over a longer period (up to 200 days), demonstrating the possibility to characterize long lasting metabolic effects of this model EDC, despite physiological and metabolic changes connected with sexual maturation and aging (Cabaton et al., 2013; Tremblay-Franco et al., 2015).

In addition to TBT, other chemicals such as DDT, BPA, phthalates or hydrocarbons present in jet fuel can also induce transgenerational obesity in rodents (Manikkam et al., 2013; Skinner et al., 2013; Tracey et al., 2013). Since most of these chemicals are not PPAR γ or RXR activators, they likely act through other mechanisms to impair metabolic regulation leading to obesity. Since the metabolomics profiles of animals ancestrally exposed to candidate obesogens had never been studied in depth, it was unknown whether metabolomics could be used to unveil the transgenerational effects of EDCs.

Here we show for the first time, results of non-targeted ^1H NMR metabolomic analyses of plasma and liver samples collected from mice ancestrally exposed to TBT. Samples were obtained from two independent transgenerational studies denoted as T2 and T3. T2 was a pilot metabolomic experiment based on plasma samples collected during our previously published study, which demonstrated that exposing mouse dams during pregnancy and lactation to a 50 nM TBT dose led to transgenerational obesity in F4 generation males without additional exposure (Chamorro-García et al., 2017). T3, detailed in this study, focused on the effects of ancestral prenatal exposure to TBT (5 or 50 nM) on the metabolome, studied in the F3 generation using a protocol specifically designed to integrate the generation of plasma and liver samples for metabolomic analyses. We also analyzed the effect of increased dietary fat challenge on the metabolome of these ancestrally TBT-exposed animals.

2. Methods

2.1. Animals

C57BL/6J mice were purchased from the Jackson Laboratory (Sacramento, CA) and housed in micro-isolator cages in a temperature-controlled room (21–22 °C) with a 12 h light/dark cycle. Water and food were provided *ad libitum* unless otherwise indicated. Animals were treated humanely and with regard for alleviation of suffering. All procedures conducted in this study were approved by the Institutional Animal Care and Use Committee of the University of California, Irvine. At the moment of euthanasia, each mouse was assigned a code, known

only to a lab member not involved in the dissection process. All tissue harvesting was performed with the dissector blinded to which groups the animals belonged.

2.1.1. Pilot experiment – TBT transgenerational experiment 2 (T2)

We performed a pilot experiment with samples isolated from an already published TBT transgenerational study designated as “T2” (Chamorro-García et al., 2017). Dams were exposed to the treatments via drinking water for 7 days prior to conception, throughout pregnancy and lactation. Treatments were removed at weaning, 21 days after birth. Blood plasma was isolated from F4 generation animals whose F0 dams were exposed to 50 nM TBT or DMSO vehicle (control animals) throughout pregnancy and lactation, at 8 and 33 weeks of age (before and after the exposure to a diet challenge), and was processed as previously described (Table 1, Chamorro-García et al., 2017). Detailed group sizes are provided in Fig. 3 legend.

2.1.2. Main experiment – TBT transgenerational experiment 3 (T3)

For this new transgenerational experiment, denoted as T3; we purchased 45 male and 90 female C57BL/6 J mice at 7 weeks of age. Female mice (30 females per treatment group) were randomly assigned to the different F0 treatment groups and exposed via drinking water to 5 nM TBT (“TBT5” group), 50 nM TBT (“TBT50” group) or 0.1% DMSO vehicle (all of which were diluted in 0.5% carboxymethyl cellulose in water to maximize solubility), for 7 days prior to mating, and was maintained throughout pregnancy (Table 1). Treatments were removed at birth. These TBT concentrations were chosen based on our previous studies (Chamorro-García et al., 2013; Chamorro-García et al., 2017; Chamorro-García et al., 2018) and are fifty and five times lower than the established no observed adverse effect level (NOAEL), respectively (Vos et al., 1990). Chemicals were administered to the dams throughout pregnancy. Sires were never directly exposed to the treatment. No statistically significant differences were observed in the number of pups or the sex ratio per litter among the different groups (Suppl. Table 1).

From each generation, we randomly chose only 1 male and 1 female per litter for endpoint analysis and another 1 male and 2 females per litter for breeding to produce the next generation. To randomize the breeding process as much as possible, we did not breed siblings and did not breed females from the same litter with the same male. Control animals were bred to each other and TBT-exposed animals were bred to each other. Animals were subjected to the diet challenge and used for metabolomics analyses. F3 animals were fasted overnight prior to euthanasia at 8 weeks or 28 weeks of age (before and after diet challenge, respectively). Blood was isolated by cardiac puncture into a heparinized syringe and treated with protease inhibitors as previously described (Chamorro-García et al., 2017). Livers were isolated, flash-frozen in liquid nitrogen and kept at -80°C until analyses. Detailed group sizes are provided in figure legends.

Diet challenge: T3 animals from both control and treatment groups were maintained on a standard diet (SD) (PicoLab 5053; 24.5% KCal from protein, 13.1% KCal from fat, and 62.3% KCal from carbohydrates) from weaning onward. On week 12, the diet was changed to a higher-fat diet (HFD) (PicoLab 5058; 23% KCal from protein, 21.6% KCal from fat, and 55.2% KCal from carbohydrates) for 8 weeks, then the diet was switched back to the SD for 8 further weeks. Body weight and body

Table 1

Comparison of experimental design of T2 and T3 studies.

	Pilot experiment (T2)	Complete experiment (T3)
Window of exposure	<i>In utero</i> & lactation	<i>In utero</i>
Treatments	DMSO, 50 nM TBT	DMSO, 5 nM TBT, 50 nM TBT
Generation analyzed	F4	F3
HFD start age (weeks)	19	12
HFD end age (weeks)	25	20
Euthanasia age (weeks)	33	28
Fasting length	4 h	Overnight (~16 h)

composition were measured weekly as previously described (Chamorro-García et al., 2017). Same diets were used for T2 but the exposure occurred at different ages as indicated in Table 1.

2.2. Chemicals (^1H NMR spectroscopy)

Methanol and dichloromethane were purchased from Scharlau SL (Sentmenat, Spain), deuterium oxide (D_2O) and sodium 3-trimethylsilyl-2,2,3,3-tetradeuteriopropionate (TSP) from Eurisotop (Saint-Aubin, France). Ultrapure water was produced using a Milli-Q system (Millipore, Saint-Quentin-en-Yvelines, France).

2.3. Sample preparation for ^1H NMR spectroscopy

Plasma samples: after thawing at 4°C and vortexing, 100 μL plasma was mixed with 150 μL phosphate buffer (0.2 M; pH 7.0) prepared in D_2O and containing 1 mM TSP. Each sample was vortexed and centrifuged for 15 min at 5000 g and 4°C , then 200 μL aliquots were transferred to standard 3 mm NMR tubes.

Liver samples: extraction procedure was derived from the method described by Beckonert et al. (Beckonert et al., 2007) using methanol/dichloromethane/water. Liver samples (100 mg) were homogenized in methanol (400 μL) and ultrapure water (85 μL) using a tissue homogenizer Fastprep-24 (MP Biomedicals, Irvine, CA, USA). 200 μL of dichloromethane were then added to the samples. After vortexing, 200 μL of dichloromethane were added to the samples. Samples were left on ice for 15 min, then centrifuged at 5000 g for 15 min at 4°C . The upper phase containing polar metabolites was removed and dried before being reconstituted in 600 μL phosphate buffer (0.2 M; pH 7.0) prepared in D_2O and containing 1 mM TSP. Samples were then transferred into 5 mm NMR tubes.

2.4. ^1H nuclear magnetic resonance (NMR) analyses

All ^1H NMR spectra were acquired at 300 K on a Bruker Avance III HD spectrometer operating at 600.13 MHz (Bruker Biospin, Rheinstetten, Germany), equipped with an autosampler and an inverse ^1H - ^{13}C - ^{15}N - ^{31}P cryoprobe. For plasma samples, ^1H NMR spectra were acquired using the Carr-Purcell-Meiboom-Gill (CPMG) spin-echo pulse sequence with presaturation, with a total spin-echo delay of 240 ms to attenuate broad signals from macromolecules. For liver aqueous extracts, ^1H NMR spectra were recorded using the noesypr1d (TOPSPIN version 3.2, Bruker Biospin) pulse sequence for water suppression and a mixing time of 100 ms. For all spectra, a total of 128 transients were collected into 32 k data points using a spectral width of 20 ppm, a relaxation delay of 2 s and an acquisition time of 1.36 s. All free induction decays were then multiplied by an exponential function with a line broadening factor of 0.3 Hz prior to Fourier transform. All spectra were referenced to the chemical shift of TSP (δ 0.0 ppm). Metabolite assignments of NMR signals were performed using 1D & 2D NMR experiments (^1H - ^1H homonuclear Correlation Spectroscopy (COSY), and ^1H - ^{13}C Single Quantum Coherence spectroscopy (HSQC)) by matching the recorded signals with NMR spectral databases (MetaboHub PeakForest database v2.0.4, <https://metabohub.peakforest.org/webapp/>; Human Metabolome Database (HMDB), <https://hmdb.ca/>).

With the CPMG NMR sequence, the broad resonances from proteins were attenuated, but lipids were still visible due to their long T_2 . Chemical shift depends on the chemical environment of the proton, and protons of similar molecules give signals with close chemical shifts. Lipid species contain many long chain fatty acids. Thus, many signals of protons overlap, and a detailed characterization of lipid species is not possible. However, the 0.84–0.90 ppm and 1.25–1.30 ppm peaks correspond to the resonance of the CH_3 and CH_2 groups, respectively, of all lipids present in LDL and VLDL.

2.5. Data reduction and multivariate statistical analyses

All NMR spectra were manually phase- and baseline-corrected using TOPSPIN (V3.5, Bruker Biospin, Germany), then data were reduced using AMIX (version 3.9, Bruker, Analytik) to integrate 0.01 ppm wide regions corresponding to the δ 8.5–0.5 and δ 9.5–0.5 ppm region, respectively, for plasma samples and aqueous liver extracts. The δ 5.1–4.5 ppm region, which includes the water resonance, was excluded for both matrices. The δ 3.68–3.63 and 1.20–1.16 and δ 3.0–2.5 ppm regions, which include ethanol and DMSO resonances, respectively, were excluded for plasma samples. The δ 5.6–5.4 ppm region, which includes the residual dichloromethane resonance, was excluded for liver extracts. A total of 685 and 821 NMR buckets were included in the plasma and liver data matrices. To account for differences in sample amount, each integrated region was normalized to the total spectral area. Multivariate analyses were used to study the effect of the treatment (Control/TBT) on the metabolome. Firstly, Principal Components Analysis (PCA) was performed to reveal intrinsic clusters and detect eventual outliers. Partial least squares–discriminant analysis (PLS-DA) was then used to model the relationship between treatment-group and NMR data. Prior PLS-DA modelling, Orthogonal Signal Correction (OSC) (Wold et al., 1998) was applied to remove confounding variability, *ie*

variability not linked to the treatment (physiological, experimental or instrumental variability). Filtered data were mean-centered or Pareto-scaled. For all score plots, Hotelling’s T2 statistics were used to construct 95% confidence ellipses. The R²Y parameter represents the explained variance. Seven-fold cross validation was used to determine the number of latent variables to include in the PLS-DA model and to estimate the predictive ability (or predicted variance, Q² parameter) of the fitted model. PLS-DA models with Q² value higher than 0.4 were considered valid (McCombie et al., 2009). In addition, the robustness of the PLS-DA models was assessed using a permutation test (number of permutations = 200). In the permutation plot, a Q² intercept < 0.05 indicates a robust model (Lapins et al., 2008). Discriminant variables were determined using the VIP (Variable Importance in the Projection) value, a global measure of the influence of each variable on the PLS components. Variables with VIP > 0.8 were considered discriminant. Finally, significance of relative integration difference between treatment groups was tested based on the non-parametric Wilcoxon or Kruskal-Wallis test (depending on the number of treatment groups). The Benjamini-Hochberg (BH) procedure for the false discovery rate (FDR) was applied to take into account multiple testing. NMR variables with FDR-adjusted p-value < 0.05 were considered significantly different (Benjamini et al., 2001). SIMCA-P software (V14, Umetrics AB, Umea,

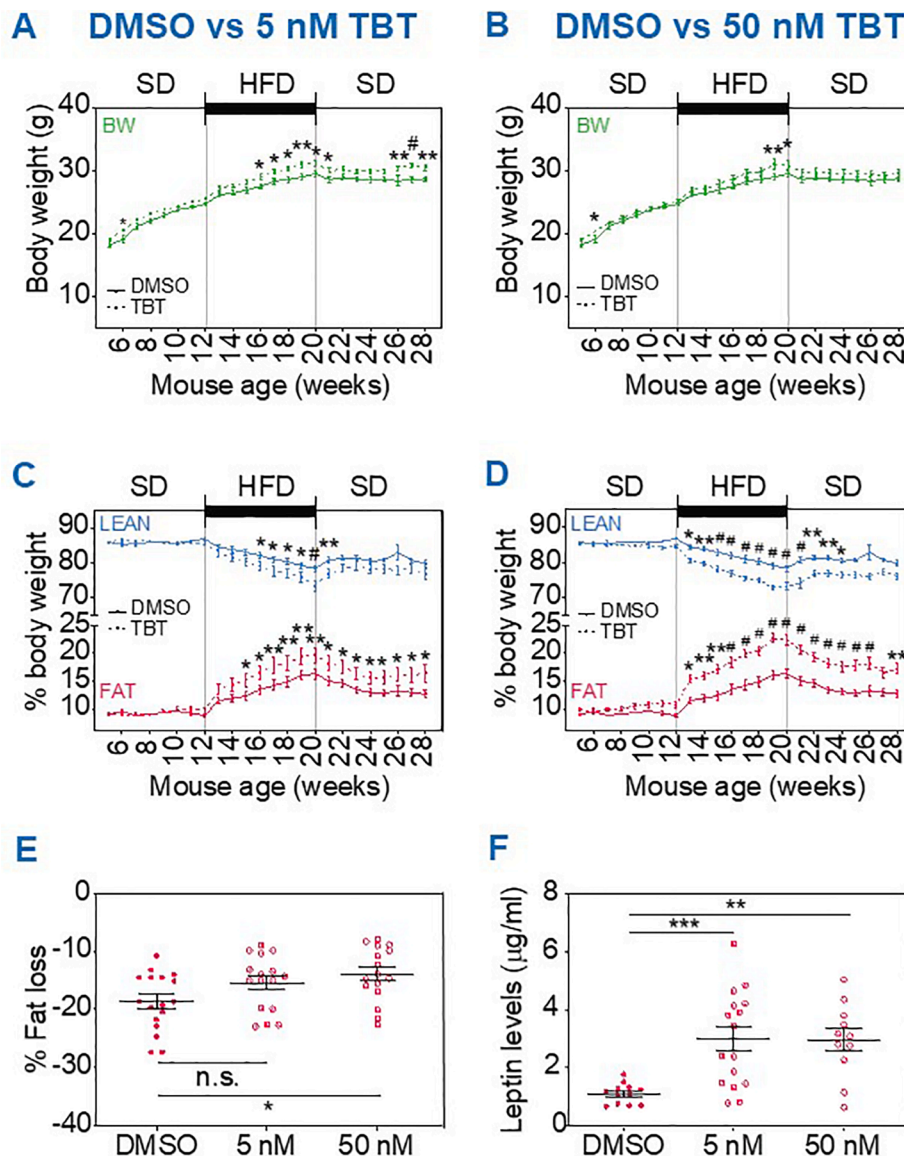


Fig. 1. Obesity phenotype in male mice ancestrally exposed to TBT. Weekly body weight and body composition in animals ancestrally exposed to 5 nM TBT (A, C) and 50 nM TBT (B, D) compared to control group (DMSO). (E) Percentage of body fat loss after ~16 h of fasting at 28 weeks of age. (F) Plasma levels of leptin at 28 weeks of age. Statistical significance was determined by two-way ANOVA followed by Dunnett’s post-test in panels A–D. Statistical significance was determined by Kruskal-Wallis test followed by Dunn’s post-test in panels E–F. Data are presented as mean ± s.e.m. *p < 0.05, **p < 0.01, #p < 0.001. BW: Body Weight; SD: Standard diet; HFD: Higher fat diet. Panels A–E: Control n = 17, TBT5 n = 16, TBT50 n = 16; for panel F: Control n = 12, TBT5 n = 16, TBT50 n = 11.

Sweden) was used to perform the multivariate analyses and R (<https://www.r-project.org/>) for univariate testing.

3. Results

3.1. Ancestral exposure to TBT leads to metabolic disruption

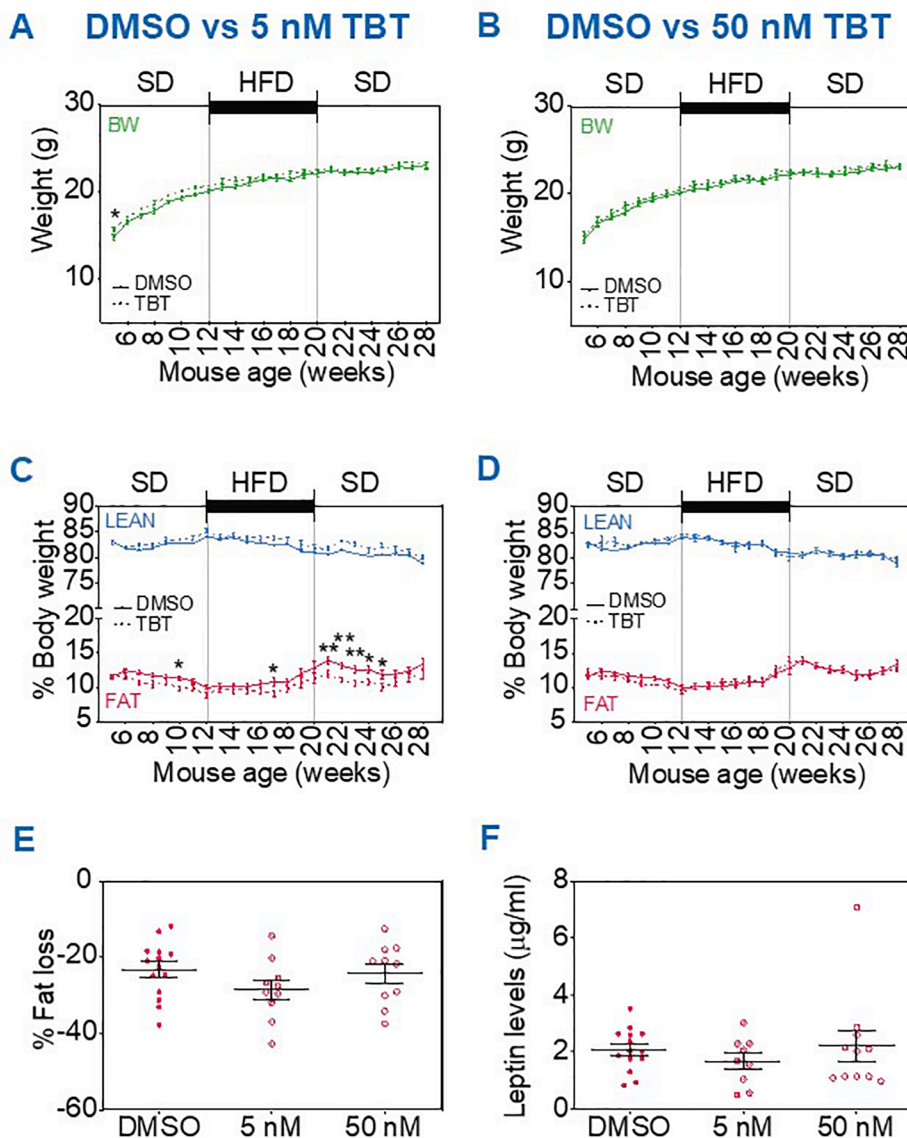
In the new T3 experiment (main experiment) detailed in this paper, effects of ancestral TBT exposure throughout pregnancy on standard parameters in the F3 generation, such as body weight and composition, were confirmed to be much stronger in male than in female mice, similarly to our previous findings (Chamorro-García et al., 2013; Chamorro-García et al., 2017). Male F3 animals ancestrally exposed to TBT accumulated significantly more fat after the diet was changed from the SD to the HFD at 12 weeks of age. Compared to control animals, the average total weight of F3 males ancestrally exposed to TBT became significantly higher starting from week 19 (TBT50 group, Fig. 1B) and as early as week 16 for the lowest dose (TBT5 group, Fig. 1A). While total weight gain did not remain significantly higher in F3 animals from the TBT50 group after their return to a standard diet at week 20, a significant increase in body weight was observed in the TBT5 group until week 21, and during the latest stages of the study (weeks 26 and onwards,

Fig. 1A).

Ancestrally-exposed male F3 mice displayed a significantly higher fat storage initiated soon after the beginning of the diet challenge, irrespective of TBT dose at the expense of lean mass (Fig. 1C, D). The increased body fat persisted through the end of the study, even after returning to the standard diet. The effect was slightly more pronounced in the TBT50 group. In addition, exposed animals were not able to mobilize this fat as rapidly as control animals when fasting. After the final overnight fasting at week 28, the percentage of fat loss was significantly lower for TBT50 mice (Fig. 1E). Plasma analyses revealed significantly increased leptin levels in male mice ancestrally exposed to either concentration of TBT compared to control animals (Fig. 1F).

For F3 female mice we found no effect on total body weights before, during or after the diet challenge at either TBT dose (Fig. 2A, B). However, in females from the TBT5 group, a small, but significant decrease in fat accumulation was observed between weeks 21 and 25, immediately after the end of the diet challenge (Fig. 2C). This effect did not remain significant at later stages of the study (weeks 26–28), nor was it observed in female mice from the TBT50 group (Fig. 2D). In contrast to males, no effect of ancestral TBT exposure on the capacity of female mice to mobilize fat after the final overnight fasting at week 28 was observed and plasma leptin levels were not altered (Fig. 2E, F).

Fig. 2. Obesogenic phenotype in female mice ancestrally exposed to TBT. Weekly body weight and body composition in animals ancestrally exposed to 5 nM TBT (A, C) and 50 nM TBT (B, D) compared to control group (DMSO). (E) Percentage of body fat loss after ~16 h of fasting at 28 weeks of age. (F) Plasma levels of leptin at 28 weeks of age. Statistical significance was determined by two-way ANOVA followed by Dunnett's post-test in panels A–D. Statistical significance was determined by Kruskal-Wallis test followed by Dunn's post-test in panels E–F. Data are presented as mean ± s.e.m. *p < 0.05, **p < 0.01. BW: Body Weight; SD: Standard diet; HFD: Higher fat diet. Panels A–E: Control n = 14, TBT5 n = 10, TBT50 n = 10; Panel F: Control n = 14, TBT5 n = 9, TBT50 n = 10.



3.2. Plasma metabolomic profiles in F4 males and females (T2)

We used remaining plasma samples from our previously published transgenerational study (T2) in a pilot experiment to assess whether any changes in metabolites could be identified in plasma isolated from F4 animals ancestrally exposed to 50 nM TBT or 0.1% DMSO (vehicle) throughout pregnancy and lactation (Chamorro-García et al., 2017). In ^1H NMR metabolomics analyses of plasma from 8-week old animals (before the diet challenge), most statistical analyses generated PLS-DA models with two latent components (Fig. 3), characterized by faithful representations of the data (R^2Y) backed by high cumulative predictive capacity scores (Q^2) (see Suppl. Tables 2–3).

At week 8, a strong discrimination of ancestrally exposed (versus control) mice was observed. For females (Fig. 3B), the R^2Y (percentage of the inter-individual variance explained by the treatment) was 95.3%, and the calculated Q^2 score (cumulative predictive capacity) of 0.804 was indicative of a very robust model. Accordingly, the score plot of the PLS-DA analysis showed a marked separation between control and TBT groups; 21 variables had a VIP value >0.8 and were statistically different by the Kruskal-Wallis test after Benjamini-Hochberg FDR correction. These variables corresponded to 3 metabolites (2D-NMR spectra identification), namely isoleucine and creatine, decreased in the plasma of TBT50 8-week old F4 females, and glucose, which was increased compared to control animals. A marked discrimination of control versus ancestrally exposed mice was also observed in males (Fig. 3A), with extremely high scores ($R^2Y = 99.1\%$; $Q^2 = 0.978$); 6 variables had a VIP value >0.8 and were significantly different (FDR corrected-p value of the Wilcoxon test). These corresponded to a single metabolite, lactate, decreased in animals ancestrally exposed to TBT.

At week 33 (after the diet challenge), multivariate analysis could only discriminate F4 males ancestrally exposed to TBT from controls (Fig. 3C), with 5 discriminant and significant variables, corresponding

again to a single metabolite (lactate), which at that time-point was found to be increased in ancestrally exposed animals. For females, no robust model could be generated (Fig. 3D). However, only a limited number of female plasma samples was available at 33 weeks ($n = 5$), which limited the statistical power of the PLS-DA analysis and could explain this latter result. A key inference from this experiment is that both males and females in the TBT group differed from controls before the diet challenge, indicating that the diet challenge itself was not the cause of the differences we previously observed after the diet challenge (Chamorro-García et al., 2017).

3.3. Plasma and liver metabolomic profiles in F3 mice (T3)

The promising results and robust models generated by PLS-DA analyses for the T2 pilot experiment prompted us to perform a more extensive metabolomic analysis in a new and independent transgenerational study. In this study (T3), F0 dams were exposed only during pregnancy, either to 5 or 50 nM TBT, and animals were analyzed in the F3 generation (Table 1). Samples were used to seek discriminant ^1H NMR metabolomic fingerprints in F3 males and females before (8 weeks; plasma, Fig. 4) and after (28 weeks; plasma and liver, Fig. 5) the diet challenge (further detailed in Suppl. Tables 2–3).

3.3.1. ^1H NMR metabolomics reveal marked differences in both sexes

In males, PLS-DA analysis performed on the whole data set of 3 experimental groups (controls, TBT5, TBT50) generated, for plasma, a model with 1 latent component characterized by a fair percentage of the inter-individual variability explained ($R^2Y = 46.3\%$) and a fair cumulative predictive capacity ($Q^2 = 0.421$) (Fig. 4A). The score plot of the PLS-DA analysis showed a discrimination between TBT50 animals and a cluster comprising both control TBT5 animals. Four metabolites (glutamine, dimethylsulfone, pyruvate and 3-hydroxybutyrate) as well

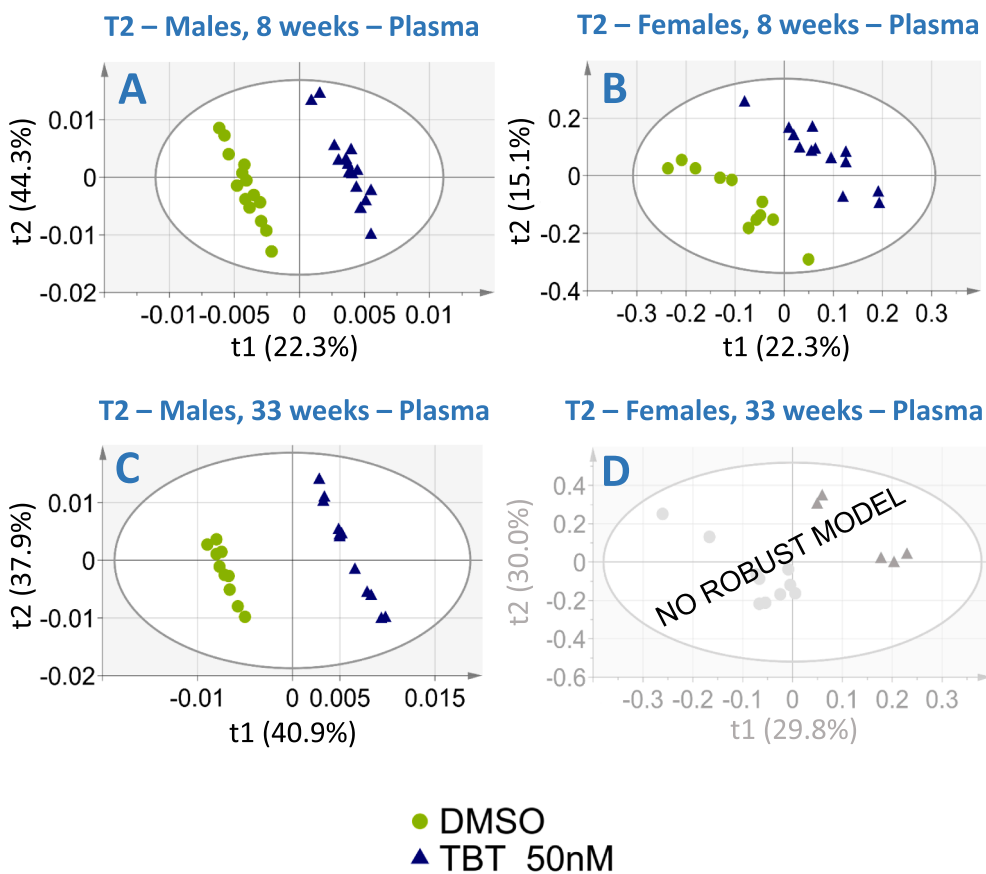


Fig. 3. Two-dimensional PLS-DA scores plot of T2 study plasma samples integrated ^1H NMR spectra at 8 (top) and 33 (bottom) weeks of age. Left column: Male samples; Right column: Female samples. Each dot represents an observation (animal), projected onto first (horizontal axis) and second (vertical axis) PLS-DA components. Groups are shown in different symbols and colors. The black ellipse determines the 95% confidence interval, which is drawn using Hotelling's T2 statistic. A. 8-weeks male samples (Control: $n = 14$, TBT50: $n = 15$, 2 latent components, $R^2Y = 95.3\%$, $Q^2 = 0.80$). B. 8-weeks female samples (Control: $n = 12$, TBT50: $n = 14$, 2 latent components, $R^2Y = 99.1\%$, $Q^2 = 0.98$). C. 33-weeks male samples (Control: $n = 10$, TBT50: $n = 12$, no robust model). D. 33-weeks female samples (Control: $n = 5$, TBT50: $n = 12$, 2 latent components, $R^2Y = 99.8\%$, $Q^2 = 0.99$).

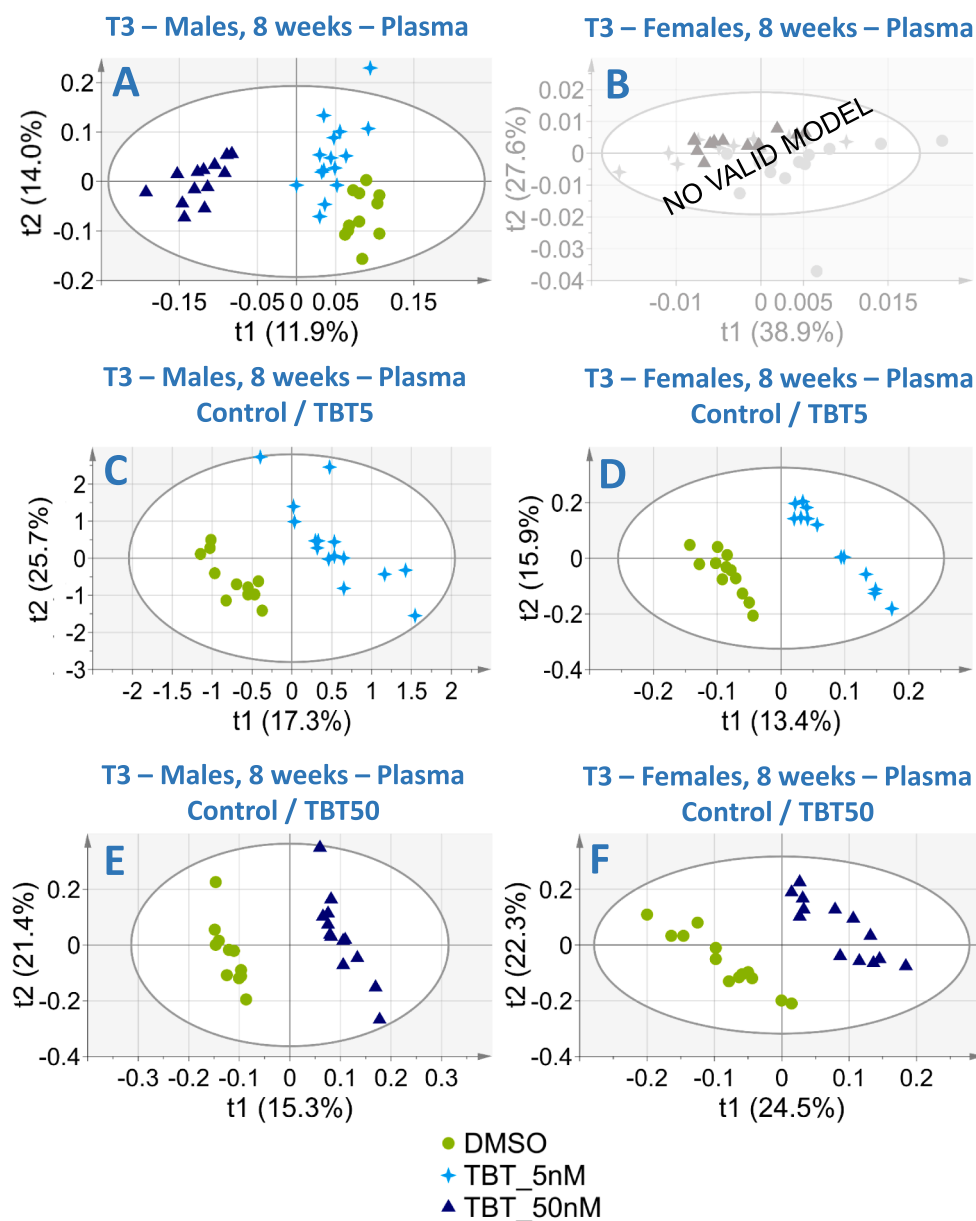


Fig. 4. Two-dimensional PLS-DA scores plot of T3 study plasma samples integrated ^1H NMR spectra at 8 weeks of age. Left column: Male samples; Right column: Female samples. Each dot represents an observation (animal), projected onto first (horizontal axis) and second (vertical axis) PLS-DA components. Groups are shown in different symbols and colors. The black ellipse determines the 95% confidence interval, which is drawn using Hotelling's T^2 statistic. A. All male samples (Control: $n = 11$, TBT5: $n = 15$, TBT50: $n = 13$, 1 latent component, $R^2Y = 46.3\%$, $Q^2 = 0.42$). B. All female samples (Control: $n = 13$, TBT5: $n = 13$, TBT50: $n = 13$, no valid model). C. Control/TBT5 male samples (Control: $n = 11$, TBT5: $n = 15$, 2 latent components, $R^2Y = 90.6\%$, $Q^2 = 0.74$). D. Control/TBT5 female samples (Control: $n = 12$, TBT5: $n = 13$, 2 latent components, $R^2Y = 98.4\%$, $Q^2 = 0.84$). E. Control/TBT50 male samples (Control: $n = 11$, TBT50: $n = 13$, 2 latent components, $R^2Y = 98.2\%$, $Q^2 = 0.90$). F. Control/TBT50 female samples (Control: $n = 13$, TBT50: $n = 13$, 2 latent components, $R^2Y = 95.9\%$, $Q^2 = 0.92$).

as lipids (LDL and VLDL) were found to be responsible for the discrimination between the 2 clusters (as identified from 37 variables having a VIP value > 0.8 , and with a median statistically different with the Kruskal–Wallis test; Fig. 6). Further pairwise PLS-DA analyses demonstrated strong discrimination between male mice ancestrally exposed either to TBT5 (Fig. 4C) or TBT50 (Fig. 4F) and controls. Both models were robust and valid, based on very high percentages of the variability explained by the treatment (R^2Y ; 90.6 and 98.2, respectively) backed by high Q^2 scores (0.74 and 0.90, respectively). In addition to glutamine, dimethylsulfone and 3-hydroxybutyrate (all confirmed to be decreased in both TBT groups), the plasma metabolites responsible for discriminating ancestral TBT effects in these pairwise comparisons, were lysine and pyruvate (decreased only in TBT50 animals), lipids and glucose (increased in the same group) and betaine, specifically decreased in TBT5 mice only (Fig. 6). Although several diagnostic biomarkers were similar for the two ancestral TBT doses, TBT effects appeared to be more pronounced for the higher dose with additional metabolites being modulated in TBT50 mice.

In females, although no valid model could be generated when analyzing all groups together (Fig. 4B), pairwise comparisons

demonstrated a distinct discrimination between exposed and non-exposed animals. Transgenerational effects of both TBT5 (Fig. 4D; R^2Y : 98.4, Q^2 : 0.84) and TBT50 (Fig. 4F; R^2Y : 95.9, Q^2 : 0.82), compared with control animals, were demonstrated by robust and valid PLS-DA models. Both were found to rely on changes in lipids (decreased) and 3-hydroxybutyrate levels, which was increased in TBT50 females (same as in males) but decreased in TBT5 animals (Fig. 6). Lipids were decreased in females for both ancestral TBT doses (conversely to males). Leucine was also a discriminant metabolite, increased in TBT50 female mice only.

3.3.2. Long lasting dose- and sex-dependent transgenerational effects

At 28 weeks of age, 8 weeks after the end of HFD and return to SD, animals were euthanized following overnight fasting. Plasma and liver samples were analyzed using ^1H NMR metabolomics. Score plots of the 4 PLS-DA analyses using the entire data sets demonstrated a marked discrimination between ancestrally exposed and non-exposed animals for plasma and liver samples in both males and females, all with robust and valid models (Fig. 5). However, the metabolites responsible for the discrimination between groups were mostly different in males and

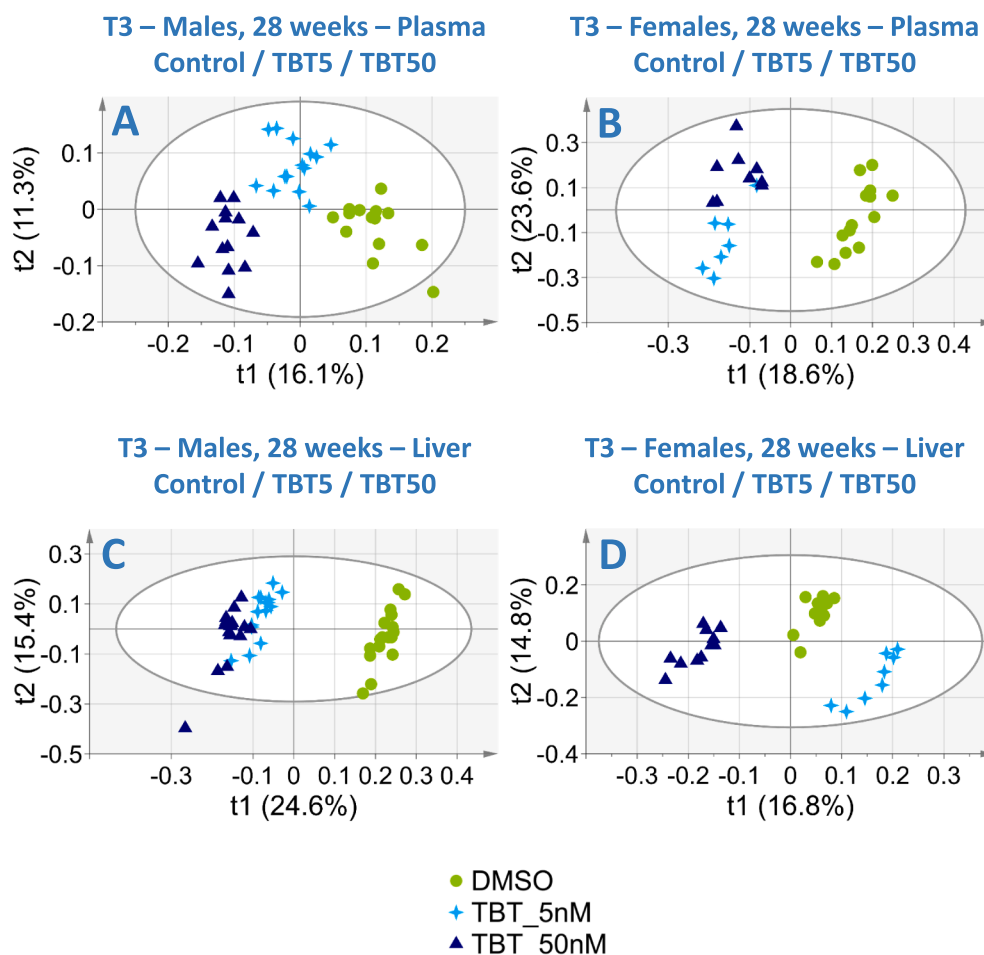


Fig. 5. Two-dimensional PLS-DA scores plot of T3 study plasma samples (top) and liver extracts (bottom) integrated ^1H NMR spectra at 28 weeks of age. Left column: Male samples; Right column: Female samples. Each dot represents an observation (animal), projected onto first (horizontal axis) and second (vertical axis) PLS-DA components. Groups are shown in different symbols and colors. The black ellipse determines the 95% confidence interval, which is drawn using Hotelling's T2 statistic. A. Male plasma samples (Control: $n = 14$, TBT5: $n = 14$, TBT50: $n = 13$, 4 latent components, $R^2Y = 95.5\%$, $Q^2 = 0.86$). B. Female plasma samples (Control: $n = 14$, TBT5: $n = 7$, TBT50: $n = 9$, 2 latent components, $R^2Y = 70.5\%$, $Q^2 = 0.52$). C. Male liver extracts (Control: $n = 17$, TBT5: $n = 16$, TBT50: $n = 16$, 1 latent component, $R^2 = 48.9\%$, $Q^2 = 0.49$). D. Female liver extracts (Control: $n = 13$, TBT5: $n = 8$, TBT50: $n = 11$, 4 latent components, $R^2 = 98.0\%$, $Q^2 = 0.95$).

females. For each sex, the list of discriminating metabolites (Fig. 6) was also generally more extensive for the TBT50 than the TBT5 group, although several discriminating metabolites were common to both doses.

For plasma samples, most of the inter-group variability was explained by ancestral exposure to TBT (males: Fig. 5A, $R^2Y = 95.5\%$ and $Q^2 = 0.86$, 4 latent components; females: Fig. 5B, $R^2Y = 70.5\%$ and $Q^2 = 0.52$, 2 latent components). Both male and female TBT5/TBT50 animals were successfully separated from controls along the first (horizontal) axis. Animals ancestrally exposed to TBT5 versus TBT50 were further discriminated along the second (vertical) axis. Increased ketone bodies were among plasma metabolites contributing to the discrimination between groups (Fig. 6). For TBT50 versus controls, this was the case for acetate (males), 3-hydroxybutyrate (females) and acetoacetate (both). Acetone was increased in TBT5 animals compared to controls for both males and females. In parallel, glucose was a discriminant variable, decreased in males and females ancestrally exposed to the TBT50 dose, compared to controls.

Several amino acids were also identified as discriminant parameters in plasma metabolic profiles. Similar trends were observed for males and females, with glycine and lysine levels being increased in both TBT50 groups. However, differential response in plasma was observed for glutamine, which was decreased in males but increased in females. Notably, branched-chain amino acids (BCAA) were discriminant metabolites of TBT ancestral exposure: leucine and valine in TBT50 males, and isoleucine in TBT5 females, all 3 were increased in plasma samples.

A marked sexually dimorphic response was also evidenced in lipids from plasma samples: they were increased in males and decreased in females ancestrally exposed to TBT (both doses) compared to controls.

Finally, endogenous metabolite variations in plasma included lactate, which was decreased only in males (both ancestral TBT doses). In the T2 pilot study (based on a limited number of samples) lactate had already been identified as a key biomarker metabolite in males, for which it was similarly decreased at 8 weeks in F4 generation mice, but increased after the diet challenge.

PLS-DA analyses carried out on liver samples from T3 animals and based on whole datasets (controls, TBT5, TBT50) confirmed strong and lasting effects of ancestral TBT exposure. Two-dimensional score plot in males (Fig. 5C) showed a marked separation between controls and F3 mice ancestrally exposed to TBT, with a valid and robust model ($R^2Y = 48.9\%$, $Q^2 = 0.479$). For females (Fig. 5D), all 3 experimental groups were readily discriminated along axis 1, with a valid and robust model ($R^2Y = 98.0\%$, $Q^2 = 0.94$).

Liver metabolites contributing to the discrimination between groups are summarized in Fig. 6. Hepatic glucose was increased in all ancestrally exposed mice except in TBT5 females, where it was decreased. Interestingly, TBT5 females were the only group for which we observed a decrease in body fat percentage (Fig. 2C), and for which changes in other discriminant metabolites in liver (glucose, glycerol, glycine, lysine, taurine and choline) were systematically opposite to all other groups (Fig. 6). Except for glucose, the profiles of altered metabolites were very different for males and females. For females, these profiles were also very different according to the ancestral exposure dose, whereas for males many metabolites that were modulated in the TBT5 group were also found to be modulated in the TBT50 group (Fig. 6).

Choline was a discriminant metabolite of ancestral TBT exposure and was significantly decreased for both TBT5 and TBT50 males compared to controls. In the same groups, creatine and glutathione were decreased as

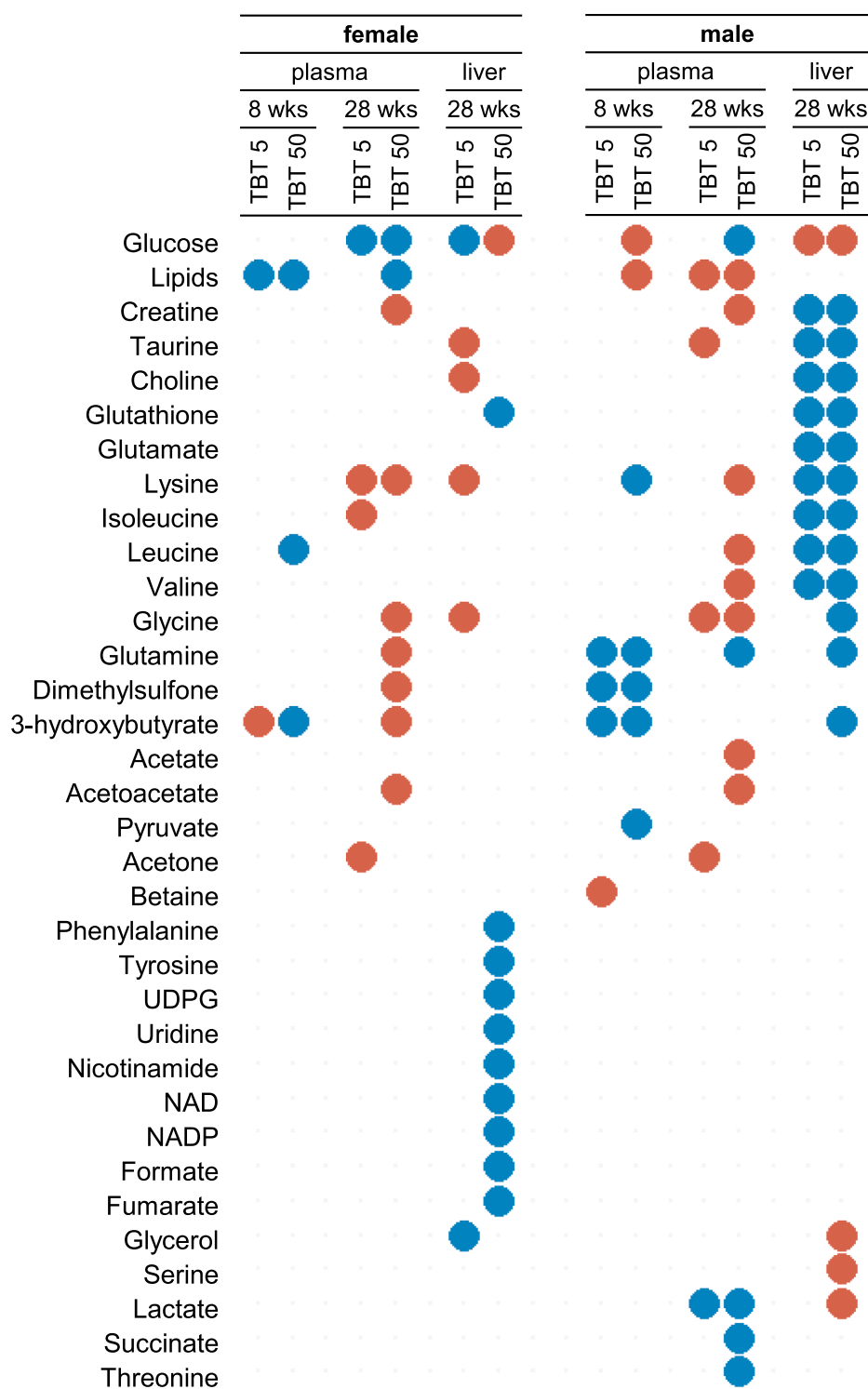


Fig. 6. Discriminant metabolites identified in plasma and liver extract samples from the pairwise comparison of PLS-DA models (after OSC filtration) for control vs TBT (5 or 50 nM) exposed groups, for male and female mice, at 8 weeks and 28 weeks, respectively. Metabolites with a VIP value > 0.8 and with significant difference between exposed and control groups (FDR corrected p-value < 0.05 based on the Wilcoxon test) were considered as discriminant and are displayed. Blue dots indicate a decrease in metabolite level in TBT exposed groups (TBT 5 or 50 nM) compared to control animals, red dots indicate an increase in metabolite level in TBT exposed groups compared to control animals.

well. A similar decrease of glutathione was observed for females, but solely for the TBT50 group. Glycerol and lactate were additional discriminant metabolites, but only in TBT50 males (Fig. 6).

All BCAA were found to be discriminant metabolites in the livers of males ancestrally exposed to TBT: leucine, isoleucine and valine were decreased in TBT5 as well as TBT50 males. In addition, lysine and taurine were both decreased in these groups (Fig. 6). Glutamine (decreased) and serine (increased) were also discriminants metabolites, but only in TBT50 males. Conversely, phenylalanine and tyrosine were found to be decreased after ancestral exposure only in TBT50 females.

Further specific changes were observed in the liver metabolome of TBT50 females. First, nicotinamide, nicotinamide adenine dinucleotide (NAD) and nicotinamide adenine dinucleotide phosphate (NADP) were discriminant metabolites, decreased in TBT50 female livers, suggesting a major metabolic dysregulation. Second, both uridine diphosphate glucose (UDPG) as well as its precursor uridine were decreased in these TBT50 females (compared to controls or to TBT5 females). Notably, glutathione was also a discriminant metabolite of ancestral TBT exposure in TBT50 females as well as TBT50 and TBT5 males (Fig. 6).

4. Discussion

Obesity and related diseases have become an important health and economic burden worldwide (Hales et al., 2017). Studies performed in animal models showed that exposures to environmental factors such as obesogens during critical windows of development contributed to increased fat storage not only in the directly exposed F1 and F2 offspring, but also in the F3-F4 generations that were not directly exposed to the environmental agent (reviewed in Heindel and Blumberg, 2019). Identifying biomarkers of ancestral exposure would allow one to ascertain which individuals might be predisposed to suffering the effects of such exposure even before phenotypic effects could be observed.

Pioneering *in vivo* ^1H NMR-metabolomics studies carried out with the model xenoestrogen bisphenol A (BPA) revealed that perinatal exposure led to lasting alterations in blood and tissue metabolomes in F1 rodents exposed during gestation through weaning (Cabaton et al., 2013; Tremblay-Franco et al., 2015). However, these studies were carried out in the F1 generation only, whereas several EDCs were shown to drive lasting changes, including metabolic changes, through multiple generations (reviewed in Heindel and Blumberg, 2019; Lee and Blumberg, 2019). NMR spectroscopy is among the main techniques used in metabolomic studies. It is nondestructive, easily quantifiable, highly automatable and exceptionally reproducible, making NMR-based metabolomics a robust approach to highlight metabolic disturbances. NMR is particularly amenable to detecting compounds that LC-MS cannot detect, such as sugars, organic acids, alcohols, polyols, and other highly polar compounds (Emwas et al., 2019). TBT, an environmental pollutant, RXR and PPAR γ activator was demonstrated to drive lasting transgenerational metabolic effects in mice up to the 4th generation after F0 exposure (Chamorro-García et al., 2017; Diaz-Castillo et al., 2019). Here we performed a ^1H NMR-metabolomic exploration of TBT effects based on two independent transgenerational experiments. The main study (T3) focused on plasma and hepatic liver metabolomes of F3 generation mice whose F0 ancestors were exposed to 5 or 50 nM TBT throughout pregnancy. This study was preceded by a pilot experiment (T2) based on a limited number of plasma samples from F4 generation animals whose F0 ancestors were exposed to 50 nM TBT throughout pregnancy and lactation, still available from our published work (Chamorro-García et al., 2017; Diaz-Castillo et al., 2019).

Remaining T2 plasma samples were analyzed by ^1H NMR, to assess the feasibility of using metabolomic analysis to determine whether the metabolome of F4 animals was impacted by ancestral TBT exposure. PLS-DA analyses of NMR integrated spectra demonstrated a strong discrimination of ancestrally-exposed F4 animals versus controls at 8 weeks (before HFD challenge), with valid and robust models characterized by high $R^2\text{Y}$ (percentage of variability explained by the exposure) and Q^2 scores (predictive capability of the model), both for males and females. At 33 weeks (after HFD challenge), a valid and robust discrimination was demonstrated again for males ancestrally exposed to TBT, but not for females (no valid model, possibly due to the limited number of available plasma samples for this group). These new metabolomic results are consistent with our published *in vivo* data for the same animals where only males exhibited increased white adipose tissue (WAT) weight after HFD challenge (Chamorro-García et al., 2017). Although limited by the sample size, this pilot ^1H NMR experiment demonstrated that metabolomics could be used to investigate transgenerational effects of TBT exposure. ^1H NMR revealed a marked difference between ancestrally TBT exposed mice and controls prior to HFD exposure, demonstrating that despite the lack of measurable changes in body weight and composition at that stage (Chamorro-García et al., 2017), early metabolic modulation had already taken place in these animals. Some of the observed metabolic changes preceded the HFD challenge.

The T3 study confirmed that ancestral TBT exposure during F0 pregnancy led to marked transgenerational effects on the phenotype and physiology of F3 male descendants. Total weight gain and body

composition were altered at both ancestral TBT doses. This effect was revealed or exacerbated by the HFD challenge. Total body weights of male F3 mice whose F0 dams were exposed to TBT increased more rapidly during the HFD challenge period compared to vehicle exposed F0 dams. Weight differences became significant over the last 3 weeks of the diet challenge in males ancestrally exposed to 50 nM TBT, and 3 weeks earlier in animals ancestrally exposed to 5 nM TBT. Longitudinal analysis of body composition further highlighted the metabolic disruption triggered by ancestral TBT exposure. At both TBT doses, MRI analysis of F3 males demonstrated a marked difference in fat accumulation, beginning during the HFD challenge and lasting until the end of the experiment (28 weeks).

These results are consistent with our published T2 work in F4 mice ancestrally exposed to TBT during gestation and lactation. There, it was demonstrated that males gained substantial body fat upon HFD challenge, did not readily mobilize this fat during fasting and exhibited elevated serum leptin levels and elevated expression of leptin mRNA in WAT (Chamorro-García et al., 2017). These data were interpreted as indicating that these animals exhibited a leptin-resistant, “thrifty phenotype” (Chamorro-García et al., 2017). In the new T3 experiment, similar effects on body fat, fat mobilization and elevated serum leptin levels were confirmed in F3 males but not females. F3 females appeared to be much less sensitive to ancestral TBT exposure, based on body weight curves (irrespective of dose) or even on MRI results (50 nM TBT: no effect). However, in females whose F0 dams were exposed to the lowest TBT dose (5 nM) a significant reduction of body fat percentage was observed, especially during the 5 weeks following the diet challenge, markedly contrasting with the effects observed in males. This confirmed our previous results about male-specific transgenerational effects of TBT with regards to body weight and fat content, this time in F3 mice ancestrally exposed solely *in utero*, and at two different, environmentally-relevant TBT doses: 50 nM and 5 nM.

^1H NMR metabolomics experiments and subsequent PLS-DA modeling on T3 samples unequivocally demonstrated significant effects of ancestral TBT exposure on both plasma and liver metabolomes. This was true by the end of the study (28 weeks) for male as well as female mice, but marked metabolic disorders were already found to exist prior to the diet challenge (8 weeks) despite the absence of overt differences in body weight and composition. Although earlier time-points were not examined, it cannot be ruled out that ^1H NMR metabolomics might have unveiled the effects of ancestral exposure to TBT before 8 weeks of age. A similar approach applied to neonate mice prenatally exposed to BPA previously demonstrated such a possibility at post-natal days 2 (whole body) and 21 (tissues, although only F1 animals were examined (Cabaton et al., 2013). Transgenerational effects of TBT on the metabolome were demonstrated both in males and females, but the analysis of discriminant metabolites revealed that the effects were distinct in males and in females. Obesogenic effects consistent with body parameter results were observed in males. Although, these effects were not seen in females, ancestral TBT exposure was demonstrated to drive lasting disruptive effects on other metabolic functions.

The observation that male mice ancestrally exposed to TBT accumulated more fat (revealed by MRI) at both ancestral TBT doses was reflected by NMR metabolomics on plasma samples, with global lipids (LDL, VLDL) largely contributing to the discrimination between ancestrally exposed animals and controls at 28 weeks. Although MRI results were not conclusive at 8 weeks, ^1H NMR metabolomics discriminated male mice from controls at both doses, with lipids being among the main discriminant plasma variables between exposed and control male mice, for the highest ancestral dose.

Following overnight fasting at 28 weeks, glucose was found to be among the main metabolomic variables contributing to the discrimination between controls and ancestrally exposed animals. Glucose was decreased in plasma but increased in liver for the highest ancestral TBT dose groups (males and females). Glucose was also increased in liver for the lowest TBT dose (males only). Two additional variables and

potential substrates of gluconeogenesis (lactate and glycerol) were also discriminants for effects of the highest TBT dose. Both were increased in male mice livers. Thus, in males ancestrally exposed to TBT, metabolomic analyses suggested a deep impairment of carbohydrate metabolism.

The production of glucose from glycogen was likely significantly impaired in F3 mice, because of the marked reduction of their lean mass (including muscles) revealed by MRI. Effects of ancestral TBT exposure on body composition were more pronounced for the highest dose. This may explain why plasma glucose was a discriminant metabolite (decreased) for the highest dose exposure group only. Therefore, the capability of ancestrally TBT50 exposed males to increase their glucose production through the use of glycogen (lean mass loss) or from fatty acids (impaired lipid mobilization) may have been insufficient. Alternative gluconeogenesis pathways involving glucogenic amino acids were mobilized, as illustrated by glutamine and glycine, perhaps as an attempt to regulate this status. Both of these were discriminant variables decreased in the livers of male mice ancestrally exposed to TBT50. Isoleucine was increased at both TBT doses. In females, distinct glucogenic amino acids (tyrosine and phenylalanine) were decreased in the livers of TBT50 animals only.

Metabolomic analysis demonstrated that other energy production pathways were activated in ancestrally exposed mice. At 28 weeks, several variables responsible for the marked intergroup discriminations observed in plasma were identified as ketone bodies. This was true for all ancestrally exposed animals, although qualitative differences were observed according to the dose and gender. Acetone was a discriminant metabolite of the TBT5 groups in both sexes. For ketone bodies, acetate was male specific, 3-hydroxy-butyrate was female specific, and acetoacetate was a discriminant metabolite for both sexes at the TBT50 dose; all were increased. Under fasting conditions, physiological ketosis is a normal response to low glucose availability, with ketones providing alternative energy resources. But the differential response of control versus ancestrally TBT-exposed animals indicated that homeostasis of energy metabolism was deeply disrupted in the TBT groups.

The transgenerational obesogenic effects of TBT in F3 mice were again demonstrated to be male specific. Despite that females did not gain fat or show elevated leptin levels, metabolomics unequivocally demonstrated major transgenerational effects of TBT in F3 females as well. Changes in metabolic pathways linked with energy production and use (ketosis) occurred, although body weight and composition in TBT50 F3 females were not different from controls. In females ancestrally exposed to TBT5, slight fat loss was observed. Metabolomic results were mostly distinct from those observed in males, possibly because these non-obese females had lower fat reserves than males. Glucose production heavily relies on the use of fatty acids; therefore, lower fat reserves can result in severe metabolic problems. This is supported by plasma discriminant metabolites; lipids were significantly decreased in females at 8 weeks (both doses) and at 28 weeks (TBT50 only). Liver metabolomics revealed a major dysregulation of general metabolism (nicotinamide, NAD, NADP) as well as more specific pathways (uridine, UDPG) all being discriminant metabolites decreased only in females. This suggests that TBT has broad transgenerational effects as a metabolic disruptor. The decrease of both UDPG and its precursor uridine hint at disorders in energy metabolism (UDPG is a glycogen precursor) and at specific disorders linked with phase II conjugation reactions, since UDPG is also the precursor of uridine diphosphate glucuronic acid (UDPGA), which is involved in the glucuronic acid conjugation of both endogenous and exogenous molecules. Glutathione was also a discriminant metabolite of ancestral TBT exposure, decreased in TBT50 females and in both TBT5 and TBT50 male F3 livers. Glutathione is a molecule of paramount importance as an antioxidant and also plays a major role in phase II reactions where it reacts with electrophilic compounds and/or their activated metabolites. In summary, metabolomics demonstrated a major dysregulation of metabolic pathways, including metabolites directly related to the activity of phase II metabolizing enzymes involved

in the detoxification of xenobiotics and in physiological processes (including the sensitive conjugation/deconjugation balance of natural hormones, relying on UDPGTs). Although females were not impacted by the obesogenic effects of TBT, they could be more broadly affected than males as regards their biotransformation capacities and could be more sensitive to a concomitant exposure to other EDCs due to lower UDPGT-related xenobiotics clearance. Both ancestrally exposed females (TBT50) and males (TBT5 and TBT50) could also be more sensitive to reactive xenobiotics due to glutathione depletion.

Additional metabolites that discriminated transgenerational effects of TBT, particularly in male mice, deserve special attention. Plasma metabolomics demonstrated that two BCAA (valine, leucine) were discriminant variables increased in TBT50 males. In parallel, leucine, isoleucine and valine (males, both doses) were discriminant variables decreased in the liver. Current human metabolomics research suggests that BCAAs are valuable diagnostic and prognostic plasma biomarkers of cardiometabolic diseases, including obesity and metabolic syndrome, although the mechanisms underlying the relationship of plasma BCAA to disease processes require further clarification (Siomkajlo and Daroszewski, 2019).

Liver metabolomics also demonstrated a specific decrease of choline in males, at both ancestral TBT doses. Liver is a central organ in the metabolism of this essential nutrient and major precursor of phospholipids and neurotransmitters. Severe choline deficiency can cause muscle damage and was reported to play a role in the onset and progression of NAFLD. We note that the lean mass of ancestrally TBT-treated F3 males (including muscles) was significantly decreased and that we previously reported NAFLD in F1-F3 generations of ancestrally TBT treated animals in both sexes (Chamorro-García et al., 2013). In humans, metabolomic biomarkers related to choline status could help predict individuals at risk of NAFLD (Corbin and Zeisel, 2012). In ancestrally exposed male mice, choline deficiency combined with the obesogenic effects of TBT may enhance NAFLD susceptibility. Choline availability depends on food intake and on its *de novo* synthesis via the phosphatidylethanolamine N-methyl-transferase (PEMT) pathway (Wortmann and Mayr, 2019). Several possible reasons may explain decreased choline in male livers. Insufficient supply from diet is likely ruled out because no similar decreases were observed in females or in controls, and major inter-individual genetic differences in the PEMT pathway are unlikely in C57BL/6J mice. However, the PEMT gene is known to be estrogen-inducible in humans (Zeisel, 2006) as well as mice (Noga and Vance, 2003), which could have contributed to the gender specific effects we observed. Another possibility is that since many bacteria of the gut microbiome actively use choline (Sherriff et al., 2016), its bioavailability might be impaired in ancestrally exposed males despite adequate dietary supply. This could indicate transgenerational effects of TBT on the composition of the gut microbiome, which has not yet been examined. Since choline is a precursor of S-adenosyl methionine (SAM), which is essential for methylation reactions, the modulation of hepatic choline status could impact gene expression and epigenetic regulation. This is consistent with recent results for ancestrally TBT-exposed mice (T2 experiment), in which males were demonstrated to be predisposed to obesity due to altered chromatin organization that biased DNA methylation and gene expression (Chamorro-García et al., 2017; Diaz-Castillo et al., 2019).

In conclusion, our new results confirm the transgenerational male-specific obesogenic effects of TBT, previously observed in F4 animals ancestrally exposed during gestation and lactation (Chamorro-García et al., 2017; Diaz-Castillo et al., 2019). Here, a similar response of F3 males was observed even at a ten-fold lower TBT dose, and despite that ancestral exposure only occurred during gestation. This study represents the first application of metabolomics to the transgenerational effects of EDC exposure, based on plasma and liver sampling. A major and somewhat dose-dependent impact of ancestral TBT exposure on metabolism was demonstrated in F3 male mice. The results provided solid clues about potential targets and mechanisms for future analysis. These

data support the need for further investigation using a multi-omics strategy (including specific lipidomics), with subsequent bioinformatics modeling, to characterize the underlying metabolic pathways modulated by TBT and to determine its precise mode of action. This study also unequivocally demonstrated major transgenerational effects of TBT in female mice. These involved changes in homeostasis of energy metabolism as well as a deep impairment of biotransformation capacity, which may affect the ability of these animals to detoxify xenobiotics and to sustain a normal endogenous metabolism, including the preservation of their hormonal balance.

CRedit authorship contribution statement

Raquel Chamorro-García: Conceptualization, Methodology, Investigation, Resources, Writing – original draft, Writing – review & editing, Formal analysis, Visualization. **Nathalie Poupin:** Methodology, Data curation, Formal analysis, Writing – original draft, Writing – review & editing, Visualization, Validation. **Marie Tremblay-Franco:** Methodology, Investigation, Data curation, Validation, Formal analysis, Data curation, Writing – original draft, Visualization. **Cécile Canlet:** Methodology, Investigation, Data curation, Validation, Formal analysis, Data curation, Writing – original draft, Visualization. **Riann Egusquiza:** Investigation. **Roselyne Gautier:** Investigation, Resources. **Isabelle Jouanin:** Investigation, Data curation. **Bassem M. Shoucri:** Investigation. **Bruce Blumberg:** Conceptualization, Funding acquisition, Project administration, Supervision, Methodology, Investigation, Writing – original draft, Writing – review & editing, Formal analysis, Validation. **Daniel Zalko:** Methodology, Writing – original draft, Writing – review & editing, Formal analysis, Conceptualization, Investigation, Data curation, Supervision.

Declaration of Competing Interest

The authors declare the following financial interests/personal relationships which may be considered as potential competing interests: B. Blumberg is a named inventor on U.S. patents 5,861,274; 6,200,802; 6,815,168; and 7,250,273 related to PPAR γ . All other authors declare they have no actual or potential competing financial interests.

Acknowledgements

This work was supported by a grant from the NIH (ES023316) to B.B. The authors thank all members of the Blumberg laboratory for their technical assistance during dissections.

Data sharing

Raw data, experimental parameters, annotations and identities are deposited in the open source repository Metabolights hosted by the European Bioinformatics Institute (EBI), accession number MTBLS2455. The complete dataset can be accessed here: <https://www.ebi.ac.uk/metabolights/MTBLS2455>.

Appendix A. Supplementary material

Supplementary data to this article can be found online at <https://doi.org/10.1016/j.envint.2021.106822>.

References

Beckonert, O., Keun, H.C., Ebbels, T.M., Bundy, J., Holmes, E., Lindon, J.C., et al., 2007. Metabolic profiling, metabolomic and metabonomic procedures for nmr spectroscopy of urine, plasma, serum and tissue extracts. *Nat. Protoc.* 2, 2692–2703.
Benjamini, Y., Drai, D., Elmer, G., Kafkafi, N., Golani, I., 2001. Controlling the false discovery rate in behavior genetics research. *Behav. Brain Res.* 125, 279–284.

Cabaton, N.J., Canlet, C., Wadia, P.R., Tremblay-Franco, M., Gautier, R., Molina, J., et al., 2013. Effects of low doses of bisphenol a on the metabolome of perinatally exposed cd-1 mice. *Environ. Health Perspect.* 121, 586–593.
Cano-Sancho, G., Salmon, A.G., La Merrill, M.A., 2017. Association between exposure to p, p'-ddt and its metabolite p, p'-dde with obesity: integrated systematic review and meta-analysis. *Environ. Health Perspect.* 125, 096002.
Chamorro-Garcia, R., Sahu, M., Abbey, R.J., Laude, J., Pham, N., Blumberg, B., 2013. Transgenerational inheritance of increased fat depot size, stem cell reprogramming, and hepatic steatosis elicited by prenatal exposure to the obesogen tributyltin in mice. *Environ. Health Perspect.* 121, 359–366.
Chamorro-Garcia, R., Diaz-Castillo, C., Shoucri, B.M., Kach, H., Leavitt, R., Shioda, T., et al., 2017. Ancestral perinatal obesogen exposure results in a transgenerational thrifty phenotype in mice. *Nat. Commun.* 8, 2012.
Chamorro-Garcia, R., Shoucri, B.M., Willner, S., Kach, H., Janesick, A., Blumberg, B., 2018. Effects of perinatal exposure to dibutyltin chloride on fat and glucose metabolism in mice, and molecular mechanisms, in vitro. *Environ. Health Perspect.* 126, 057006.
Corbin, K.D., Zeisel, S.H., 2012. Choline metabolism provides novel insights into nonalcoholic fatty liver disease and its progression. *Curr Opin Gastroenterol* 28, 159–165.
Diaz-Castillo, C., Chamorro-Garcia, R., Shioda, T., Blumberg, B., 2019. Transgenerational self-reconstruction of disrupted chromatin organization after exposure to an environmental stressor in mice. *Sci. Rep.* 9, 13057.
Emwas, A.H., Roy, R., McKay, R.T., Tenori, L., Saccenti, E., Gowda, G.A.N., et al., 2019. Nmr spectroscopy for metabolomics research. *Metabolites* 9.
Emwas, A.M., Salek, R.M., Griffin, J.L., Merzaban, J., 2013. Nmr-based metabolomics in human disease diagnosis: applications, limitations, and recommendations. *Metabolomics* 9, 1048–1072.
Gore, A.C., Chappell, V.A., Fenton, S.E., Flaws, J.A., Nadal, A., Prins, G.S., et al., 2015. Edc-2: The endocrine society's second scientific statement on endocrine-disrupting chemicals. *Endocr. Rev.* 36, E1–E150.
Grun, F., Watanabe, H., Zamanian, Z., Maeda, L., Arima, K., Cubacha, R., et al., 2006. Endocrine-disrupting organotin compounds are potent inducers of adipogenesis in vertebrates. *Mol. Endocrinol.* 20, 2141–2155.
Hales, C., Carroll, M., Fryar, C.D., Ogden, C.L., 2017. Prevalence of obesity among adults and youth: United states, 2015–2016. (NCHS Data Brief). NCHS Data Brief No 288, October 2017. Hyattsville, MD:U.S. Department of Health & Human Services.
Heindel, J.J., Blumberg, B., 2019. Environmental obesogens: Mechanisms and controversies. *Annu. Rev. Pharmacol. Toxicol.* 59, 89–106.
Kanayama, T., Kobayashi, N., Mamiya, S., Nakanishi, T., Nishikawa, J., 2005. Organotin compounds promote adipocyte differentiation as agonists of the peroxisome proliferator-activated receptor gamma/retinoid x receptor pathway. *Mol. Pharmacol.* 67, 766–774.
Kim, S., Li, A., Monti, S., Schlezinger, J.J., 2018. Tributyltin induces a transcriptional response without a brite adipocyte signature in adipocyte models. *Arch. Toxicol.* 92, 2859–2874.
Kirchner, S., Kieu, T., Chow, C., Casey, S., Blumberg, B., 2010. Prenatal exposure to the environmental obesogen tributyltin predisposes multipotent stem cells to become adipocytes. *Mol. Endocrinol.* 24, 526–539.
Lapins, M., Eklund, M., Spjuth, O., Prusis, P., Wikberg, J.E., 2008. Proteochemometric modeling of hiv protease susceptibility. *BMC Bioinf.* 9, 181.
Lee, M.K., Blumberg, B., 2019. Transgenerational effects of obesogens. *Basic Clin. Pharmacol. Toxicol.* 125 (Suppl 3), 44–57.
Li, X., Ycaza, J., Blumberg, B., 2011. The environmental obesogen tributyltin chloride acts via peroxisome proliferator activated receptor gamma to induce adipogenesis in murine 3t3-l1 preadipocytes. *J. Steroid Biochem. Mol. Biol.* 127, 9–15.
Locke, A.E., Kahali, B., Berndt, S.I., Justice, A.E., Pers, T.H., Day, F.R., et al., 2015. Genetic studies of body mass index yield new insights for obesity biology. *Nature* 518, 197–206.
Ludwig, D.S., Hu, F.B., Tappy, L., Brand-Miller, J., 2018. Dietary carbohydrates: Role of quality and quantity in chronic disease. *BMJ* 361, k2340.
Manikkam, M., Tracey, R., Guerrero-Bosagna, C., Skinner, M.K., 2013. Plastics derived endocrine disruptors (bpa, dehp and dbp) induce epigenetic transgenerational inheritance of obesity, reproductive disease and sperm epimutations. *PLoS ONE* 8, e55387.
McCombie, G., Browning, L.M., Titman, C.M., Song, M., Shockcor, J., Jebb, S.A., et al., 2009. Omega-3 oil intake during weight loss in obese women results in remodelling of plasma triglyceride and fatty acids. *Metabolomics* 5, 363–374.
Milton, F.A., Lacerda, M.G., Sinoti, S.B.P., Mesquita, P.G., Prakasan, D., Coelho, M.S., et al., 2017. Dibutyltin compounds effects on ppargamma/txralpha activity, adipogenesis, and inflammation in mammalian cells. *Front. Pharmacol.* 8, 507.
Newbold, R.R., Padilla-Banks, E., Jefferson, W.N., 2009. Environmental estrogens and obesity. *Mol. Cell. Endocrinol.* 304, 84–89.
Noga, A.A., Vance, D.E., 2003. A gender-specific role for phosphatidylethanolamine n-methyltransferase-derived phosphatidylcholine in the regulation of plasma high density and very low density lipoproteins in mice. *J. Biol. Chem.* 278, 21851–21859.
Regnier, S.M., El-Hashani, E., Kamau, W., Zhang, X., Massad, N.L., Sargis, R.M., 2015. Tributyltin differentially promotes development of a phenotypically distinct adipocyte. *Obesity (Silver Spring)* 23, 1864–1871.
Riu, A., McCollum, C.W., Pinto, C.L., Grimaldi, M., Hillenweck, A., Perdu, E., et al., 2014. Halogenated bisphenol-a analogs act as obesogens in zebrafish larvae (danio rerio). *Toxicol. Sci.* 139, 48–58.
Sena, G.C., Freitas-Lima, L.C., Merlo, E., Podratz, P.L., de Araujo, J.F., Brandao, P.A., et al., 2017. Environmental obesogen tributyltin chloride leads to abnormal hypothalamic-pituitary-gonadal axis function by disruption in kisspeptin/leptin signaling in female rats. *Toxicol. Appl. Pharmacol.* 319, 22–38.

- Sherriff, J.L., O'Sullivan, T.A., Properzi, C., Oddo, J.L., Adams, L.A., 2016. Choline, its potential role in nonalcoholic fatty liver disease, and the case for human and bacterial genes. *Adv Nutr* 7, 5–13.
- Shoucri, B.M., Martinez, E.S., Abreo, T.J., Hung, V.T., Moosova, Z., Shioda, T., et al., 2017. Retinoid x receptor activation alters the chromatin landscape to commit mesenchymal stem cells to the adipose lineage. *Endocrinology* 158, 3109–3125.
- Shoucri, B.M., Hung, V.T., Chamorro-García, R., Shioda, T., Blumberg, B., 2018. Retinoid x receptor activation during adipogenesis of female mesenchymal stem cells programs a dysfunctional adipocyte. *Endocrinology*.
- Siomkajlo, M., Daroszewski, J., 2019. Branched chain amino acids: passive biomarkers or the key to the pathogenesis of cardiometabolic diseases? *Adv. Clin. Exp. Med.* 28, 1263–1269.
- Skinner, M.K., Manikkam, M., Tracey, R., Guerrero-Bosagna, C., Haque, M., Nilsson, E.E., 2013. Ancestral dichlorodiphenyltrichloroethane (ddt) exposure promotes epigenetic transgenerational inheritance of obesity. *BMC Med.* 11, 228.
- Tontonoz, P., Spiegelman, B.M., 2008. Fat and beyond: the diverse biology of ppargamma. *Annu. Rev. Biochem.* 77, 289–312.
- Tracey, R., Manikkam, M., Guerrero-Bosagna, C., Skinner, M.K., 2013. Hydrocarbons (jet fuel jp-8) induce epigenetic transgenerational inheritance of obesity, reproductive disease and sperm epimutations. *Reprod. Toxicol.* 36, 104–116.
- Tremblay-Franco, M., Cabaton, N.J., Canlet, C., Gautier, R., Schaeberle, C.M., Jourdan, F., et al., 2015. Dynamic metabolic disruption in rats perinatally exposed to low doses of bisphenol-a. *PLoS ONE* 10, e0141698.
- Vos, J.G., De Klerk, A., Krajnc, E.I., Van Loveren, H., Rozing, J., 1990. Immunotoxicity of bis(tri-n-butyltin)oxide in the rat: effects on thymus-dependent immunity and on nonspecific resistance following long-term exposure in young versus aged rats. *Toxicol. Appl. Pharmacol.* 105, 144–155.
- Watt, J., Schlezinger, J.J., 2015. Structurally-diverse, ppargamma-activating environmental toxicants induce adipogenesis and suppress osteogenesis in bone marrow mesenchymal stromal cells. *Toxicology* 331, 66–77.
- Watt, J., Baker, A.H., Meeks, B., Pajevic, P.D., Morgan, E.F., Gerstenfeld, L.C., et al., 2018. Tributyltin induces distinct effects on cortical and trabecular bone in female c57bl/6j mice. *J. Cell. Physiol.* 233, 7007–7021.
- Wold, S., Antii, H., Lindgren, F., Ohman, J., 1998. Orthogonal signal correction of near-infrared spectra. *Chemomet. Intell. Lab. Syst.* 44, 175–185.
- World Health Organization, 2020. Noncommunicable diseases. Obesity data and statistics. Available: <http://www.euro.who.int/en/health-topics/noncommunicable-diseases/obesity/data-and-statistics> (accessed June 5 2020).
- Wortmann, S.B., Mayr, J.A., 2019. Choline-related-inherited metabolic diseases-a mini review. *J. Inherit. Metab. Dis.* 42, 237–242.
- Zalko, D., Soto, A., Canlet, C., Tremblay-franco, M., Jourdan, F., Cabaton, N.J., 2016. Bisphenol A Exposure Disrupts Neurotransmitters Through Modulation of Transaminase Activity in the Brain of Rodents. *Endocrinology*. <https://doi.org/10.1210/en.2016-1207>.
- Zeisel, S.H., 2006. Choline: critical role during fetal development and dietary requirements in adults. *Annu. Rev. Nutr.* 26, 229–250.
- Zoeller, R.T., Brown, T.R., Doan, L.L., Gore, A.C., Skakkebaek, N.E., Soto, A.M., et al., 2012. Endocrine-disrupting chemicals and public health protection: a statement of principles from the endocrine society. *Endocrinology* 153, 4097–4110.
- Zuo, Z., Chen, S., Wu, T., Zhang, J., Su, Y., Chen, Y., et al., 2011. Tributyltin causes obesity and hepatic steatosis in male mice. *Environ. Toxicol.* 26, 79–85.